Heterogeneous nucleation and depletion effect in nanowire growth

Fiqiri Hodaj, Olexii Liashenko, Andriy Gusak, Yuriy Lyashenko

Heterogeneous nucleation and depletion effect in nanowire growth

Journal:	*Philosophical Magazine & Philosophical Magazine Letters*
Manuscript ID:	TPHM-11-May-0172.R1
Journal Selection:	Philosophical Magazine
Date Submitted by the Author:	13-Jul-2011
Complete List of Authors:	Hodaj, Fiqiri; Grenoble Institute of Technology, SIMaP, CNRS-UMR 5266 Liashenko, Olexii; Cherkasy National University Gusak, Andriy; Cherkasy National University Lyashenko, Yuriy; Cherkasy National University
Keywords:	nucleation, nanowires, modelling, thermodynamics, growth
Keywords (user supplied):	step-flow kinetics

Heterogeneous nucleation and depletion effect in nanowire growth

F. Hodaj[a]*, O. Liashenko[b], A. Gusak[b] and Y. Lyashenko[b]

[a] *SIMaP - UMR CNRS 5266, Grenoble INP - UJF, BP 75, F-38402, Saint Martin d'Hères, France,* [b] *Cherkasy National University, 81 Shevchenko blvd., Cherkasy, 18031, Ukraine*
*corresponding author; e-mail: fhodaj@simap.grenoble-inp.fr

Abstract
Recent experiments of Ross, Kodambaka *et al.* proved the possibility of a mononuclear regime with heterogeneous nucleation as well as jerky growth in the VLS process for silicon nanowires. In this work, a theoretical model is presented which incorporates the effects of (i) mononuclear regime with layer by layer growth, (i) heterogeneous nucleation of each new layer at the edge of Au-Si droplet, (iii) drop of supersaturation after each successful nucleation and respective fast layer growth, (iv) time-dependent nucleation barrier during each new waiting period and (v) correlation between subsequent waiting periods (non-Markovian sequence of waiting periods).

Keywords: nucleation, nanowires, modeling, thermodynamics, growth, step-flow kinetics

1. Introduction

Development of nanotechnologies provides new problems to the theory of phase transformations - nucleation, growth and coarsening in open nanosystems.

Step-flow kinetics is one of the newest experimentally investigated features of nanowire's growth [1-3] by VLS method. Nanowires grow by rapid increasing (few milliseconds) of the nanowire's height by the value of height of one monoatomic layer with great incubation time (several seconds) between these increases. It is shown for the II-VI or III-V compounds where solubility of one component in the liquid alloy is very low that nucleation statistics is self-regulated and corresponds to sub - Poissonian distribution of waiting times between nucleation events [3] (similar idea was also suggested in [4]). In contrast, the solubility of Si in Au is very high and one would expect that self-regulation mechanism will not work in such systems. Yet, nature may not meet these expectations (see below).

Growth of sufficiently thin nanowires takes place in the mononuclear regime: for the growth of one atomic layer of the nanowire it is necessary for one nucleus to appear [5]. So, here we will limit ourselves with nanosystems in which the nucleation events proceed one by one and probability of simultaneous nucleation and of coexistence of several nuclei is negligible. Experimental results show that nucleus appears on the edge of the nanowire, on the junction of three phases: liquid, solid and vapor [2]. For the Si nanowires grown in atmosphere of low pressure of disilane it is shown that growth rate is diameter independent [6]. In this case, adsorption processes on the surface of the liquid droplet make the main contribution to the growth rate.

The following peculiarities should be taken into account in this case:

1) "Feedback" via depletion: in nanovolume even one successful nucleation and subsequent monolayer growth may cause significant depletion of whole nanosystem with one of components [7], changing the conditions (driving force) for next nucleation. In other words, system should "recover" from a previous nucleation before trying the next one.
2) Each new nucleation event proceeds in non-steady-state conditions, under rising concentration of solute supplied by external flux. So, the time dependence of the driving force should be taken into account [8].

3) Time correlation. The random nucleation process is not markovian. Each new waiting time is correlated with previous one [3]. Indeed, if previous waiting time was longer than the average one, the total number of incoming solute atoms was large, and even after consuming atoms necessary for new atomic layer, system will still have larger concentration than the average one. So, one might expect that the necessary supersaturation (for nucleation) will be reached earlier so that the next waiting time will be shorter than the average one. Thus, one might expect the negative time correlation between the nearest waiting times. Such negative time correlation should make the waiting times distribution narrower than for common markovian process without memory. We will investigate this phenomenon in detail below.

There are at least two experimental situations providing such kind of nucleation process. First is the just discovered point contact reactions between nanowires of Si and metallic (Ni, Co, Pt) nanowires or nanodots, leading to jerky (stop-and-go) epitaxial growth of silicide along the silicon nanowire, each stop meaning the waiting period for nucleation of 2d island of new silicide atomic layer [9-12]. After works of Ross, Kodambaka *et al.* we know that the same situation may be real for VLS [1,2].

Aim of this paper is just to suggest a simple model incorporating the all above mentioned peculiarities (mononuclear regime, depletion of the droplet by each nucleation event, stop-and-go kinetics and time correlation).

In the section II we present a simple model of heterogeneous nucleation of 2D island at the triple junction droplet-wire-vapor. Namely, in sub-section II.1 we find the optimal shape as a function of nucleus size (number of atoms) under the conditions of mechanical equilibrium. In sub-section II.2 we describe thermodynamics of 2D island nucleation at the bottom of the gold droplet with account of depletion caused by nucleation. At that we will take into account the depletion of the nanodroplet which can be significant even at the nucleation stage [7] and modify the Gibbs-Thomson relations for the case of complex nucleus shape. In sub-section II.3 the main equations of nucleation kinetics and lateral growth of crystalline phase are described using simple modification of Zeldovich theory. Finally, parameters of our model are presented.

In section III the results of computer experiment are presented and discussed: distribution of waiting times, time dependence of silicon concentration in liquid droplet, time correlation between subsequent waiting periods, dependence of average frequency and of average supersaturation on the flux intensity.

2. Model

Our main aim was to describe the process of layer by layer growth of nanowhisker with help of classical nucleation theory [13], at least for the realistic case of mononuclear regime. Successful nucleation of 2D islands to the new layer needs sufficient supersaturation of gold with silicon. On the other hand, after successful nucleation the new layer grows fast and takes several thousands of silicon atoms causing substantial depletion of gold droplet with silicon. (We will see below that "depletion" actually means just decrease of supersaturation, making the nucleation barrier too high for immediate next nucleation). If one takes liquid droplet as a hemisphere of radius R, then change of concentration Δc_{max} (molar fraction of silicon) due to attachment of one monolayer of atoms is about $\Delta c_{max} = -\frac{\pi R^2}{(2\pi/3)R^3} = -\frac{3}{2}\frac{h}{R}$.

Since monolayer thickness h is typically few Angstroms, the concentration change can be up to 2 percents (for R of about 20 nm). “To recover” after depletion and to make a new successful nucleation attempt, the system needs time during which whisker stands still and droplet is gradually saturated by depositing atoms.

Figure 1 here

Actually, theoretical scheme should depend on the hierarchy of characteristic times [14]. The total flux J related to deposition flux density j^{dep} just by $J= j^{dep}2\pi R^2$. First of all, one should compare the time between arrivals of new Si atoms to the droplet, $\tau_{flux}=1/J=1/(j^{dep}2\pi R^2)$, characteristic time of Si diffusion across the liquid golden droplet, $\tau_{dif}=R^2/D$, and time of atomic layer growth covering all surface after successful nucleation of 2D island, τ_{layer}. If $\tau_{flux} >> \tau_{dif}$, then we can apply thermodynamics for system "droplet plus 2D island" at fixed number of both Au and Si atoms considering Si concentration as uniform in the droplet. For nanowire (NW) radius about 20 nm and diffusivity of Si in liquid (Au,Si) alloy D about 10^{-9}m^2.s^{-1}, the critical value of depositing flux density is $j_{crit}^{dep} \approx 10^{21}$ *at*·*m*$^{-2}$*s*$^{-1}$.

We consider the possibility of stoichiometric 2D island nucleation (Fig.1) (with concentration $c_i = 1$ for the case of pure Si nanowire growth) from the supersaturated liquid solution with average Si concentration c. For this we calculate the Gibbs free energy of the system $G(x)$ at different fixed number N_{Si} of Si atoms in the droplet with N_{Au} gold atoms (or fixed average concentration $c=N_{Si}/(N_{Au}+N_{Si})$) and look for minimum of this dependence (Fig. 4a). There x is a single parameter that characterizes size of the nuclei, nucleus shape is determined, as usual, by mechanical equilibrium of surface tensions and by the place of nucleation (details will be shown below).

2.1. Nucleus shape

In our model we consider heterogeneous nucleation with the nucleus that appears on the edge of the nanowire (Fig.2). There O is the center of the nanowire's upper base, O_1 and O_2 are the centers of the internal and external curvatures of the nucleus.

Figure 2 here

The shape of the nucleus corresponds to the contour *TMPK*, which is determined by the mechanical equilibrium:

$$\begin{cases} \gamma_{i\alpha}\cos\theta_1 - \gamma_i \sin\theta_2 = 0 \\ \gamma_\alpha + \gamma_{i\alpha}\sin\theta_1 - \gamma_i\cos\theta_2 = 0 \end{cases}. \qquad (1)$$

γ_i, γ_α are the surface tensions of silicon (i) and Au-Si liquid phase (α) and $\gamma_{i\alpha}$ is the interfacial tension between silicon and liquid phase.

From (1) we can find values of the angles θ_1 and θ_2 for known values of γ_i, γ_α and $\gamma_{i\alpha}$

$$\theta_1 = arcsin\left(\frac{\gamma_i^2 - \gamma_{i\alpha}^2 - \gamma_\alpha^2}{2\gamma_\alpha\gamma_{i\alpha}}\right)$$

$$\theta_2 = arcsin\left(\frac{\gamma_{i\alpha}}{\gamma_i}cos\,\theta_1\right) \qquad (1')$$

No experimental data appear to have been published on the surface tension of solid silicon (γ_i). The evaluation of γ_i by Eustathopoulos *et al.* [15], γ_i = 1,08 J.m^{-2}, is in good agreement with the evaluation done elsewhere by Naidich et al [16].

Naidich *et al.* [17] have measured the surface tension of liquid (Au,Si) alloys in the temperature range 364 to about 1700°C. From their measurements, the surface tension of liquid alloys at T = 823K can be given approximately by the relation $\gamma_\alpha = 1 - 0{,}4c_{Si}$. For a Si-saturated liquid solution at 823K ($c_{Si} \approx 0{,}26$) the surface tension is $\gamma_\alpha \approx 0{,}9$ J.m^{-2}.

In another work, Naidich *et al.* [16] have studied the wetting of solid silicon by liquid Si-saturated (Au-Si) alloys in the temperature range 637 - 1573K. Their measurements show

that solid silicon is well wetted by liquid (Au,Si) alloys, the wetting contact angle (θ) being lower than about 50° whatever the temperature and the alloy composition. By analogy with liquid (Au,Ge)/solid-Ge system (known surface tension of solid Ge), they took the ratio γ_i/γ_α = 1,24. This assumption allows the authors to calculate interfacial tension $\gamma_{i\alpha}$ between solid silicon and Si-saturated (Au,Si) alloys from experimental values of contact angle (θ) and surface tension of (Au,Si) alloys (γ_α) as a function of temperature. At T = 823K, the interfacial tension is $\gamma_{i\alpha} \approx 0{,}4$ J.m^{-2}.

Note moreover that, in a study of anisotropy of solid Si-liquid (Al,Si) interfacial tension, Sens et al [18] have shown that the maximum anisotropy $\gamma_{i\alpha}(001)/\gamma_{i\alpha}(111)$ is about 10%. For this reason and for sake of simplicity, in the following we will use constant values of interfacial tensions at T = 823K:

$\gamma_\alpha \approx 0{,}9$ J.m^{-2} , $\gamma_i = 1{,}08$ J.m^{-2} , and $\gamma_{i\alpha} \approx 0{,}4$ J.m^{-2}.

In our model we vary the value of $HL = x$ which allows us to fix the both edges of the internal l_1 (contour TMP) and the external l_2 (contour TKP) curvatures of the nucleus. We denote the origin curvature of the nanowire bounded by these edges as l (contour TLP). For the small values of x in comparison with the radius of the nanowire R we can evaluate the length of all curvatures and the area of the nucleus:

$$l = 2\sqrt{2Rx}\,, \quad x << R \tag{2}$$

$$l_1 = \frac{2(\pi/2 - \theta_1)\sqrt{2Rx}}{\cos\theta_1}\,, \tag{3}$$

$$l_2 = \frac{2\theta_2\sqrt{2Rx}}{\sin\theta_2}\,, \tag{4}$$

$$S = 2Rx\varepsilon\,, \tag{5}$$

when ε depends only on θ_1 and θ_2:

$$\varepsilon = \frac{(\pi/2 - \theta_1 - \sin\theta_1\cos\theta_1)}{\cos^2\theta_1} + \frac{(\theta_2 - \sin\theta_2\cos\theta_2)}{\sin^2\theta_2} \tag{6}$$

Now we can write the dependence between x and the number of atoms in the nucleus n (from eq. (5) and $S = n\Omega/h$):

$$x = \frac{n\Omega}{2Rh\varepsilon} \tag{7}$$

here Ω – is the atom volume.

A calculation for reasonable parameters shows that radius O_1M of internal boundary l_1 increases more rapidly than radius O_2K of external boundary l_2, so for the small nucleus (consisting of few tens of silicon atoms) we can neglect the deviation of external boundary from initial circle, and, respectively, neglect the distortion of the droplet surface in the vicinity of the nucleation site.

2.2. Thermodynamics of nucleation and depletion in nanodroplet

a) Driving forces.

Change of Gibbs potential of the system at conditions of epitaxy can be defined as:

$$\Delta G = n\Delta g^{bulk} + \Delta G^{surf} = n\Delta g^{bulk} + \gamma_{i\alpha} l_1 h + \gamma_i l_2 h - \gamma_\alpha l h, \tag{8}$$

here h is the height of the monolayer, Δg^{bulk} is the bulk driving force per one atom of the nucleus (it is negative).

$$\Delta g^{bulk} = N/n[g(c - \Delta c) - g(c)] + g_i - g(c - \Delta c), \tag{9}$$

here $g(c)$ is the Gibbs free energy per one atom of the liquid phase (α) with concentration c, g_i is the Gibbs free energy per one atom of the solid phase with concentration $c_i = 1$ (pure

silicon), Δc is the concentration depletion after nucleus appearing, N – total amount of the atoms in droplet.

Here we use experimental data and thermodynamic assessment of Au-Si system [19,20] (see Fig.3 for the phase diagram). The Au-Si solution is modelled as liquid solution, in which the Gibbs energies are expressed as $G = \sum_{i=Au,Si} c_i G_i^0 + RT \sum_{i=Au,Si} c_i \ln c_i + G^E$, where G_i^0 - is the Gibbs energies of pure element of Au and Si at each temperature from [19] (which are reference states for Au and Si), G^E - is the excess Gibbs energy, expressed by model of subregular solution [20]. In particular, at T = 823K, the expression of G is given by the following equation:

$$G\ [J/mole] = 6702.37 \cdot c - 36320.01 \cdot (1-c) + 6842.42 \cdot \{c \cdot \ln(c) + (1-c) \cdot \ln(1-c)\} - c \cdot (1-c)\ \{36562.56 + 28464.63 \cdot (1-2c)\}$$

Figure 3 here

b) Equilibrium conditions.

We take into account the possible depletion of the droplet by the very process of 2D-nucleation. In our conditions heterogeneous nucleation occurs in volume of metastable phase of gold-silicon liquid solution. Depending on the number of Si atoms in the droplet the following situations are possible, typical for nanoparticles and nanosize diffusion zones, see for example [7,21,22]:

1) At sufficiently small number of Si atoms (relatively small c) Gibbs's free energy of the droplet has only one minimum corresponding to zero (curve (1) at Fig. 4b);
2) At larger number of Si atoms dependence $G(x)$ becomes non-monotonic with second metastable minimum (curve (2) at Fig. 4b);
3) At some critical number of Si atoms second minimum becomes stable (curve (3) at Fig. 4b);

After this the formation of new monolayer becomes thermodynamically favoured but kinetically it depends on the height of nucleation barrier. This height becomes smaller and smaller with arriving of new silicon atoms inside droplet. It means that to predict the growth characteristics we must modify Zeldovich steady-state nucleation model [13] for the case of non-stationary driving force.

Figure 4 here

c) Capillary effects

Capillary effects are usually treated in terms of curvature dependent Laplace pressure. It is appropriate in case of spherical or cylindrical surface of the nucleus, otherwise direct calculation of Laplace pressure near curved interfaces may be misleading. Actually, the capillary effect will cause the size dependence of Gibbs energy, chemical potential and of corresponding equilibrium composition. It is convenient instead of introducing individual curvatures for the different sides of the nucleus to use a single effective curvature $k^{ef} = 1/R^{ef}$, R^{ef} is the effective radius of curvature which will be introduced below.

Stable or unstable equilibrium (including saddle-point at the nucleation barrier) is determined by the condition of zero derivative of change of Gibbs energy ΔG (see eq. (8)):

$$\frac{d\Delta G}{dx} = \Delta g^{bulk} + \frac{d\Delta G^{surf}}{dn} = \Delta g^{bulk} + h\left(\gamma_{i\alpha}\frac{dl_1}{dn} + \gamma_i \frac{dl_2}{dn} - \gamma_\alpha \frac{dl}{dn}\right)$$
$$= \Delta g^{bulk} + h\frac{dx}{dn}\left(\gamma_{i\alpha}\frac{dl_1}{dx} + \gamma_i \frac{dl_2}{dx} - \gamma_\alpha \frac{dl}{dx}\right) \quad (10)$$

here γ^{ef} - is the effective surface energy coefficient (combination of $\gamma_{i\alpha}$, γ_i and γ_α, see below). We can find derivatives from (2-4) and (7):

$$\frac{dl}{dx}=\sqrt{\frac{2R}{x}},\qquad \frac{dl_1}{dx}=\frac{(\pi/2-\theta_1)\sqrt{2R}}{\cos\theta_1\sqrt{x}},\qquad \frac{dl_2}{dx}=\frac{\theta_2\sqrt{2R}}{\sin\theta_2\sqrt{x}},\qquad \frac{dx}{dn}=\frac{\Omega}{2Rh\varepsilon} \tag{11}$$

Hence,

$$\frac{d\Delta G}{dx}=\Delta g^{bulk}+\frac{\Omega}{\sqrt{2Rx\varepsilon}}\gamma^{ef}=\Delta g^{bulk}+\frac{const}{\sqrt{n}}=\Delta g^{bulk}+g_{capillar}(n) \tag{12}$$

with $$\gamma^{ef}=\frac{(\pi/2-\theta_1)}{\cos\theta_1}\gamma_{i\alpha}+\frac{\theta_2}{\sin\theta_2}\gamma_i-\gamma_\alpha. \tag{13}$$

Here $$g_{capillar}(n)=\frac{\partial\Delta G^{surf}}{\partial n}=\frac{\gamma^{ef}\Omega}{R^{ef}(n)} \tag{14}$$

with $R^{ef}(n)=\sqrt{2Rx\varepsilon}$

Thus the concentration of silicon in the droplet in equilibrium with 2D island of size n at the edge of nanowire surface may be found using standard common tangent construction (Fig. 4b) with rising the Gibbs energy g_i of the pure silicon by "Laplace term" $g_{capillar}(n)$.

The change of the value of equilibrium composition $\delta c = c_{eq}(n) - c_{eq}$ (here c_{eq} corresponds to equilibrium composition on the planar boundary) due to the appearing of curvatures on the nucleus shape should be found by using of common tangent rule (Fig.4b) is:

$$\delta c=c_{eq}(n)-c_{eq}=\frac{g_{capillar}(n)}{(1-c)g''} \tag{15}$$

here g'' is the curvature of the dependence $g_\alpha(c)$ in point c_{eq}.

From (15) we obtain:

$$\delta c=c_{eq}(n)-c_{eq}=\frac{g_{capillar}(n)}{(1-c)g''}=\frac{\gamma^{ef}\Omega}{\sqrt{2Rx\varepsilon}}\frac{1}{(1-c)g''} \tag{16}$$

2.3. Kinetics

Let's consider kinetic model of nucleation and lateral growth of nanowhisker taking into account deposition flux j^{dep} of silicon atoms (in atoms of Si per m^2 of liquid surface) from disilane gas [23]:

$$j^{dep}=\frac{P}{4kT}\sqrt{\frac{8kT}{\pi\, m_{diss}}} \tag{17}$$

here P is the disilane pressure, m_{diss} is the mass of disilane molecule (Si_2H_6).

In the following the molar fraction of silicon $c_{Si} = N_{Si}/(N_{Si} + N_{Au})$ will be noted by c.

Conservation law for silicon atoms in the droplet before nucleation gives:

$$\frac{dN_{Si}}{dt}=2\,j^{dep}\pi R^2 \tag{18}$$

The rate of change of mean concentration of silicon in the droplet before the next nucleation event is approximately equal to:

$$\frac{dc(t)}{dt}=\frac{(1-c(t))}{N_{Si}+N_{Au}}\frac{dN_{Si}}{dt}=(1-c(t))\frac{3\Omega}{R}j^{dep} \tag{19}$$

We can represent change of mean concentration of Si discretely:

$$c(t+dt)=c(t)+(1-c(t))\frac{3\Omega}{R}j^{dep} \tag{20}$$

Nucleation frequency can be defined as:

$$v(t)=e^{-\tau/t}\cdot s(G^*,x_{cr})\cdot 2\pi R \tag{21}$$

here τ is a lag-time, necessary to reach the critical size by random walk in the size space without influence of nucleation barrier, s – steady-state flux in the size space (number of

islands intersecting critical size per unit time per unit length of liquid/solid/vapor junction with the total length $2\pi R$) is taken from Zeldovich theory modified for time-dependent nucleation on the one-dimensional contour, nucleus size being determined by characteristic length x at Fig.2:

$$s = \sqrt{\frac{-\Delta G''}{\pi kT}} f^{eq}(x_{cr}) B(x_{cr}) \qquad (22)$$

here $\Delta G'' = \left(\frac{d^2 \Delta G}{dx^2}\right)_{x=x_{cr}}$ - is the curvature of the nucleation barrier, $f(x_{cr})$ - equilibrium size distribution, and diffusivity of nucleus in the size space near critical size $B(x_{cr})$ is given by:

$$B(x) = -kT \frac{\left(\frac{dx}{dt}\right)_{x \to x_{cr}}}{\left(\frac{d\Delta G}{dx}\right)_{x \to x_{cr}}} \qquad (23)$$

$$f^{eq}(x_{cr}) = const \cdot exp\left(\frac{-\Delta G(x_{cr})}{kT}\right) \qquad (24)$$

here $\Delta G(x_{cr}) = \Delta G^*$ is a nucleation barrier which previously (in Zeldovich theory) was treated as constant in time.

As we have a nucleus of pure silicon, hence, each silicon atom on the triple junction could be the centre of nucleation. So, the value of *const* in eq.(19) can be found according to receipt [24]:

$$const = \frac{c}{\Omega^{1/3}} \frac{dn}{dx} \qquad (25)$$

Indeed, if the nucleus size is characterized by number of atoms then $f(n = 1)$ is the number of silicon atoms at the perimeter $2\pi R$, equal to $c \cdot (2\pi R/\Omega^{1/3})$, divided by the length of that perimeter.

$$f^{eq}(n = 1) = \frac{c}{\Omega^{1/3}}.$$

If, instead of n, nucleus size is characterized by length x then, the distribution functions are transformed in the standard way:

$$f(x) = \frac{dn}{dx} f(n)$$

which immediately gives eq. (25).

Determination of "diffusivity in size space" $B(x_{cr})$

a) Calculation of $\left(\frac{dx}{dt}\right)_{x \to x_{cr}}$

In this paper we will limit ourselves to diffusion-controlled nucleation. Interface controlled nucleation will be considered elsewhere. Critical radius (typically about 1 nm) is assumed to be much smaller than the nanowire radius (typically ten nanometers or more), so that 2D shape of nucleus does not prevent concentration distribution to be almost spherically symmetrical. At first we use the conservation of matter considering 2D island surrounded by sphere of radius sufficiently large, so that in this radius almost hemispherical symmetry can be assumed.

Relation between total diffusion flux J^{dif} in the radial direction and the rate of nucleus growth (unusual combination of 3D diffusion with 2D particle seems OK as far as particle size is much smaller than the droplet size):

$$-J^{dif} = \frac{d}{dt}\left(\frac{Sh}{\Omega}\right) = \frac{h}{\Omega}\frac{dx}{dt}\frac{dS}{dx}, \quad (26)$$

with $J^{dif} = \eta j(\rho) 2\pi\rho^2$ at any $\rho >> x$. (27)

Factor η characterizes the deviation from the spherical geometry in the vicinity of nucleus. Unfortunately, we cannot suggest anything better than analytic solution under spherical geometry and roughly assume $\eta \approx 1/2$.

As shown in textbooks on Ham's model of precipitate growth in 3D space or for 3D-ripening [25], the steady state flux density in 3D space is:

$$j(\rho) = -\frac{D(c - c_{eq}(n))}{\Omega\rho^2} r_{min}^{ef} \quad (28)$$

here $r_{min}^{ef} = \sqrt{S/\pi}$, ($S$ is determined by eq. (5))

Moreover, from eqs. (7) and (21) we obtain:

$$\frac{dS}{dx} = 2R\varepsilon \quad (29)$$

and $$c - c_{eq}(n) = c - c_{eq} - \frac{\gamma^{ef}}{\sqrt{2Rx\varepsilon}} \frac{1}{(1-c)g''} \quad (30)$$

From combination of (26-30) we obtain the growth rate:

$$\frac{dx}{dt} = \sqrt{\frac{2\pi}{R\varepsilon}} \frac{\eta D\left[(c - c_{eq})\sqrt{x} - \frac{\Omega}{\sqrt{2R}(1-c)g''}\frac{\gamma^{ef}}{\varepsilon}\right]}{h} \quad (31)$$

Zero value of the growth rate corresponds to the critical size. Thus,

$$\frac{\Omega}{\sqrt{2R}(1-c)g''}\frac{\gamma^{ef}}{\varepsilon} = (c - c_{eq})\sqrt{x_{cr}}. \quad (32)$$

Hence,

$$\left(\frac{dx}{dt}\right)_{x\to x_{cr}} = \sqrt{\frac{2\pi}{R\varepsilon}} \frac{\eta D(c - c_{eq})\left(\sqrt{x} - \sqrt{x_{cr}}\right)}{h} \quad (33)$$

b) Calculation of $\left(\frac{d\Delta G}{dx}\right)_{x\to x_{cr}}$

From (12), with taking into account (11) and (29), we obtain:

$$\frac{d\Delta G}{dx} = \frac{d\Delta G}{dn}\frac{dn}{dx} = \left(\Delta g^{bulk} + \frac{\Omega\gamma^{ef}}{\varepsilon\sqrt{2Rx}}\right)\frac{2Rh\varepsilon}{\Omega} = \Delta g^{bulk}\frac{2Rh\varepsilon}{\Omega} + \frac{h\gamma^{ef}\sqrt{2R}}{\sqrt{x}} \quad (34)$$

Critical radius of two-dimensional nucleus corresponds to zero derivative of Gibbs energy change, thus, $\Delta g^{bulk}\frac{2Rh\varepsilon}{\Omega} = -\frac{h\gamma^{ef}\sqrt{2R}}{\sqrt{x}}$. Hence,

$$\left(\frac{d\Delta G}{dx}\right)_{x\to x_{cr}} = h\gamma^{ef}\sqrt{2R}\left(\frac{1}{\sqrt{x}} - \frac{1}{\sqrt{x_{cr}}}\right) = h\gamma^{ef}\sqrt{2R}\left(\frac{\sqrt{x_{cr}} - \sqrt{x}}{x_{cr}}\right) \quad (35)$$

Finally, after substitution of (33) and (35) in (23), we obtain:

$$B(x_{cr}) = -kT\sqrt{\frac{2\pi}{R\varepsilon}}\frac{\eta D(c - c_{eq})\left(\sqrt{x} - \sqrt{x_{cr}}\right)}{h}\cdot\frac{x_{cr}}{h\gamma^{ef}\sqrt{2R}\left(\sqrt{x_{cr}} - \sqrt{x}\right)} = kT\sqrt{\frac{\pi}{\varepsilon}}\frac{\eta x_{cr} D(c - c_{eq})}{Rh^2\gamma^{ef}} \quad (36)$$

Or, for escape from simultaneous presence of supersaturation term $(c - c_{eq})$ and critical size parameter x_{cr} we can use (32) once again:

$$B(x_{cr}) = -kT\sqrt{\frac{2\pi}{R\varepsilon}}\frac{\eta D(c-c_{eq})\left(\sqrt{x}-\sqrt{x_{cr}}\right)}{h}\cdot\frac{x_{cr}}{h\gamma^{ef}\sqrt{2R}\left(\sqrt{x_{cr}}-\sqrt{x}\right)} = kT\sqrt{\frac{\pi}{\varepsilon}}\frac{\eta x_{cr}D(c-c_{eq})}{Rh^2\gamma^{ef}}$$

$$B(x_{cr}) = kT\sqrt{\pi/2}\,\frac{\eta D\Omega}{R^{3/2}\varepsilon^{3/2}h^2(1-c)g''}\sqrt{x_{cr}} \qquad (37)$$

We determine nucleation probability and then use standard Monte Carlo scheme with eq. (21):

$$p(\Delta t) = v(t)\Delta t, \qquad (38)$$

If, at some value t^*, $random < p(\Delta t)$, then $\bar{c}_{o,i+1} = \bar{c}_i(t^*) - \frac{3h}{2R}$ (39)

Parameters and basic algorithm for modeling of step-wise nanowire growth.

Disilane pressure was changed between: $1\cdot10^{-7}$ - $3\cdot10^{-5}$ Torr (typical values used in Refs. [1,2]),
Diffusivity of Si in liquid solution $D = 10^{-9}$ m^2/s,
Height of monolayer $h = 0.31\cdot 10^{-9}$ m,
Radius of liquid droplet (taken here approximately as hemispherical) $R = 22$ nm,
Time-step was chosen depending on flux density, as one percent of anticipated average waiting time: $dt_i = \frac{<t>_i}{100} = \frac{h}{100\cdot\Omega\, j_i^{dep}}$;

A formulated model was used for numeric calculation of time behavior of supersaturation and step-flow kinetics. At that, Monte Carlo algorithm was used.

3. Results and discussion

We cannot claim to predict the mean waiting time in the steady-state regime: evidently, this average time is just an inverse total flux J ($<t>=\frac{h}{\Omega\, j^{dep}}$). Yet, one can suggest other characteristics. Typical time dependences of nucleation probability and of silicon content in gold droplet are presented on Fig.5. In particular, Fig.5b demonstrates that system possesses elements of self organization – the concentration of silicon in the droplet soon "forgets" about its initial value and fluctuates around some steady-state asymptotic value determined by the magnitude of incoming flux: the larger is the flux, the higher is the average supersaturation. Dependence of asymptotic average value of composition on incoming flux is shown in Fig.6. Time correlations between these fluctuations are discussed below.

Figure 5 here

In Figure 5b one can also see that supersaturation remains significantly larger than the depletion during one monolayer growth. Indeed, the variation of silicon concentration in the drop after nucleation and "instantaneous" growth of a silicon monolayer, for h = 0,31nm and R = 22nm, Δc_{max} = 0,0211 is twice lower than the mean silicon supersaturation $\bar{c}-c_{eq}$ of about 0,046. Thus, DEPLETION as a result of nucleation, in our previous considerations means just lower supersaturation with respectively high nucleation barrier.

Fig.6 shows that the inverse of the supersaturation decreases linearly with the logarithm of the incoming flux density (proportional to disilane pressure). This linear character of dependence can be explained by a rather simple theoretical model to be presented elsewhere.

Figure 6 here

In table 1 values of nucleation barriers energies for average silicon concentration (as well as the minimum and maximum values) are presented for different values of incoming flux. In this table values of average supersaturations are also reported. It is seen that the nucleation barrier energy decreases with the increasing incoming flux which is in agreement with the fact that silicon supersaturation increases with the deposition flux (see Fig. 6a).

In the following tables and plots we present:

Average waiting time: $< t >= \frac{\sum_{i=1}^{n} t_i}{n}$

Amount of intervals (successful nucleations) for each calculation is $n = 1000$.

Square root of average squared deviation of waiting times: $\Delta = \sqrt{\frac{\sum_{i=1}^{n} (t_i - < t >)^2}{n-1}}$

Dimensionless standard deviation: $d = \frac{\Delta}{< t >}$

Absolute time correlation: $C = \frac{\sum_{i=2}^{n} (t_i - < t >)(t_{i-1} - < t >)}{n-1}$

Dimensionless time correlation: $c = \frac{C}{\Delta} = \frac{\overline{(t_i - < t >)(t_{i-1} - < t >)}}{\overline{(t_i - < t >)^2}}$

Fig.7 gives the variation of dimensionless standard deviation and dimensionless time correlation on the logarithm of deposition flux density. The dimensionless standard deviation increases almost proportionally with the logarithm of the disilane pressure (in Torr) up to $1 \cdot 10^{-5}$ Torr whereas the variation of dimensionless time correlation presents an asymptotic behavior (i.e. for high flux densities it tends to zero).

Figure 7 here

Distributions for the disilane pressure $P = 4 \cdot 10^{-7}$, $5 \cdot 10^{-6}$ and $3 \cdot 10^{-5}$ Torr are presented on the Fig.8. They are rather well fitted by Weibull distribution. Parameters of Weibull distribution function ($y = f(x \mid a,b) = ba^{-b} x^{b-1} e^{-(\frac{x}{a})^b} I_{(0,\infty)}(x)$) are estimated. The larger is b, the narrower is distribution.

Figure 8 here

4. Summary

1. Possibility of jerky motion is confirmed in the model using assumptions of heterogeneous nucleation, mononuclear mechanism and diameter independent growth rate.
2. Zeldovich nucleation theory (including determination of diffusivity in the size space) is adapted for the case of: a) heterogenous nucleation; b) complex geometry; c) time-dependent driving force.
3. Asymptotic supersaturation of liquid Au with Si increases with increasing incoming flux. Inverse supersaturation is a linear descending function of the flux density logarithm.

4. Standard deviation of reduced waiting times distribution increases with increasing deposition flux. It correlates with time correlation for subsequent monolayers. Stronger time correlation corresponds to narrower waiting time distribution. This result obtained for silicon repeats conclusion of [3] for VLS growth of GaAs nanowhiskers.
5. Waiting time correlation for subsequent events is negative and it increases by absolute value with decreasing incoming flux. Namely, the absolute value of the dimensionless time correlation is approximately inversely proportional to the flux density.
6. Waiting time distribution is well fitted by Weibull plots with standard deviation decreasing with decreasing flux density.

Acknowledgment
Work was supported by the DNIPRO program (EGIDE - France and Ministry of Education and Science of Ukraine) and also by Ukrainian State Fund for Fundamental Research.

References

[1] C.Y. Wen, J. Tersoff, M.C. Reuter, E.A. Stach and F.M. Ross, Phys. Rev. Lett. 105 (2010) p. 195502
[2] F.M. Ross, Rep. Progr. Phys. 73 (2010) p. 114501
[3] F. Glas, J-C. Harmand and G. Patriarche. Phys. Rev. Lett. 104, (2010) p. 135501
[4] A. Gusak, A. Kovalchuk and K.N. Tu, PTM-2010, Avignon, France (2010), p. 91. Available at http://www.ffc-asso.fr/PTM2010/fichs/doc/PTM2010-Recueil_COMPLET-31-05-2010.pdf
[5] D. Kashchiev, Cryst. Growth Des. 6 (2006) p. 1154
[6] S. Kodambaka, J. Tersoff, M.C. Reuter and F.M. Ross, Phys. Rev. Lett. 96 (2006) p. 096105
[7] A.S. Shirinyan and A.M. Gusak, Phil. Mag. A 84 (2004) p. 579
[8] D. Kashchiev, Surf. Sci. 14 (1969) p. 209
[9] A.O. Kovalchuk, A.M. Gusak and K.N. Tu, Nano Lett. 10 (2010) p. 4799
[10] K-C Lu, K.N. Tu, W.W. Wu, L.J. Chen, B-Y Yoo and N.V. Myung, Appl. Phys. Lett. 90 (2007) p. 253111
[11] Y-C Lin, K-C Lu, W-W Wu, J. Bai, L.J. Chen, K.N. Tu and Y. Huang, Nano Lett. 8 (2008) p. 913
[12] Y-C Chou,W-W Wu, L-J Chen and K-N Tu. Nano Lett. 9 (2008) p. 2337
[13] L.D. Landau and E.M. Lifshitz, *Physical Kinetics, Vol. 10*, Pergamon, London, 1981
[14] V. G. Dubrovskii, N. V. Sibirev, J. C. Harmand and F. Glas, Phys. Rev. B 78 (2008) p. 235301
[15] N. Eustathopoulos, M. Nicholas, B. Drevet, *Wettability at high temperatures*, Pergamon Materials Series, v.3, Pergamon, Oxford, 1999
16. Y.V. Naidich, V.M. Perevertailo and L.P. Obushchak, Poroshkavaya Metall. 5 (1975) p. 73
[17] Y.V. Naidich, V.M. Perevertailo and L.P. Obushchak, Poroshkavaya Metall. 7 (1975) p. 63
[18] H. Sens and N. Eustathopoulos, J. Cryst. Growth 98 (1989) p. 751
[19] A.T. Dinsdale, Calphad 15 (1991) p. 317
[20] F.G.Meng, H.S. Liu, L.B. Liu and Z.P. Jin, J. Alloys Comp. 431 (2007) p. 292
[21] F. Hodaj, A. Gusak, Acta Mat. 52 (2004) p. 4305
[22] A.M. Gusak, *Diffusion-controlled Solid State Reactions*, WILEY-VCH, Weinheim, 2010

[23] K.N. Tu, *Electronic Thin-Film Reliability*, Cambridge University Press, Cambridge, 2010
[24] V.V. Slezov, J. Schmelzer J. Phys. Chem. Solids 55 (1994) 243
[25] P. Shewmon, "Diffusion in solids", TMS, Warrendale, 1992

Figure captions

Figure 1. Model system for nanowire

Figure 2. Shape of the nucleus and the directions of the surface tensions

Figure 3 The Au–Si phase diagram calculated in [20]

Figure 4. a) Dependence of thermodynamic Gibbs potential of the system during nucleation; b) Model Gibbs potentials of liquid solution and silicon (schematically);

Figure 5. Typical nucleation probability dependence on time (a) and typical silicon concentration dependence on time (b) for Si nanowires with R = 22 nm grown at T = 823 K and disilane pressure $4 \cdot 10^{-7}$ Torr.

Figure 6. Dependence of inverse supersaturation on the logarithm of disilane pressure (in Torr) for Si nanowires with R = 22 nm grown at T = 823 K.

Figure 7. Dependences of dimensionless standard deviation (a) and the logarithm dimensionless time correlation (b) on the logarithm of disilane pressure (In Torr). Note that in (b) the gradient is close to -1 which means that the absolute value of the dimensionless time correlation is approximately inversely proportional to the flux density. Phase-plane portrait of dimensionless standard deviation and dimensionless time correlation is presented (c).

Figure 8. Distribution of waiting times fitted by Weibull distribution function: for the disilane pressure $4 \cdot 10^{-7}$ Torr with parameters a = 1,045, b = 10,526 (a); for the disilane pressure $5 \cdot 10^{-6}$ Torr with parameters a = 1.052, b = 8,697 (b); for the disilane pressure $3 \cdot 10^{-5}$ Torr with parameters a = 1,064, b = 7,030 (c).

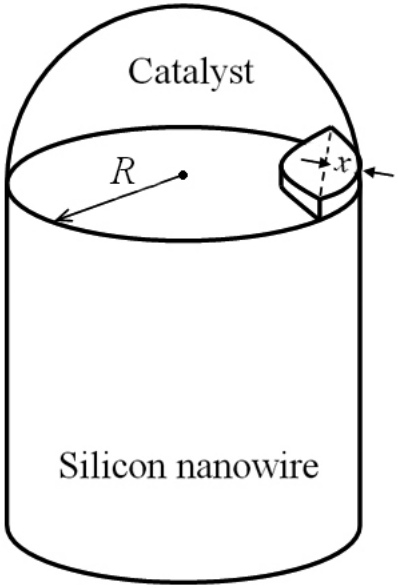

Figure 1

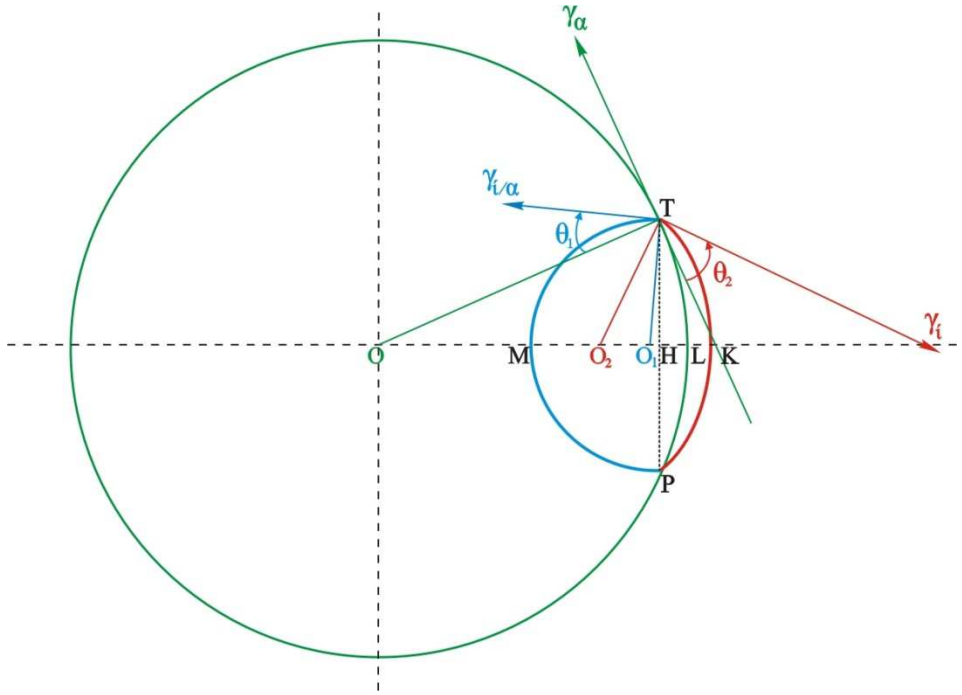

Figure 2

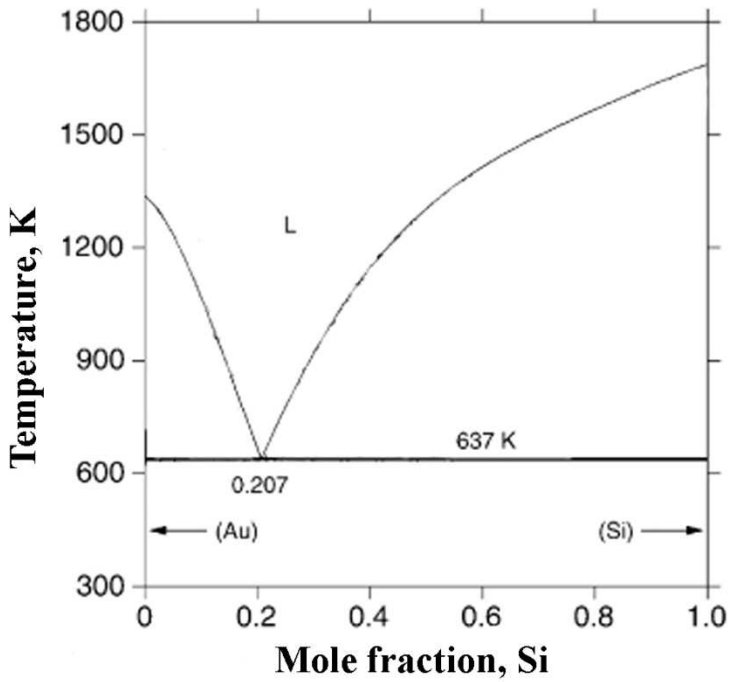
1800
1500
1200
900
600
300
Temperature, K
L
637 K
0.207
(Au)
(Si)
0
0.2
0.4
0.6
0.8
1.0
Mole fraction, Si

Figure 3

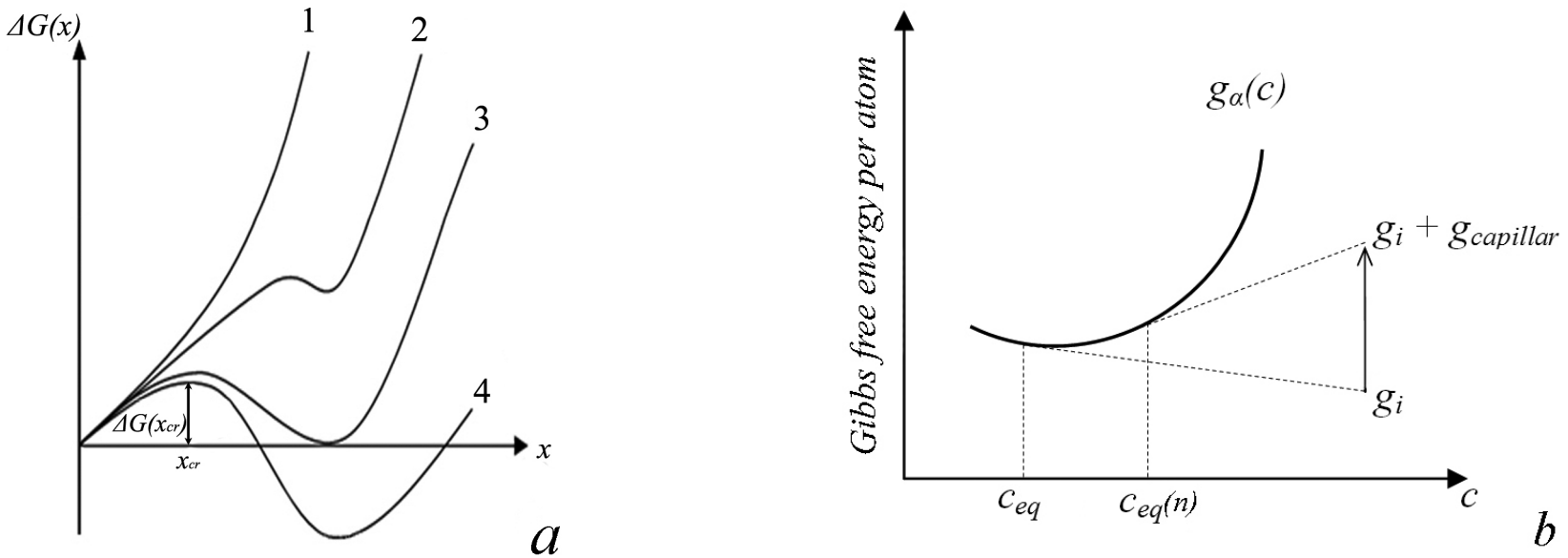
ΔG(x)
1
2
3
4
ΔG(xcr)
xcr
x
a
Gibbs free energy per atom
gα(c)
gi + gcapillar
gi
ceq
ceq(n)
c
b

Figure 4

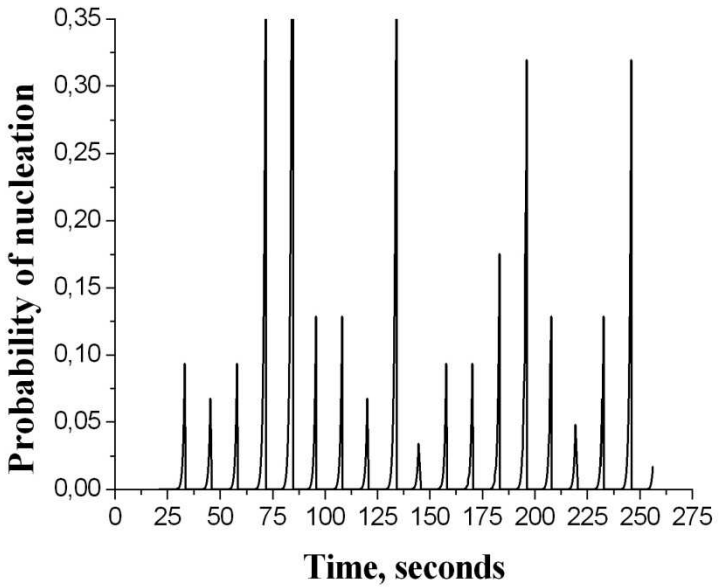
Probability of nucleation
0,35
0,30
0,25
0,20
0,15
0,10
0,05
0,00
0 25 50 75 100 125 150 175 200 225 250 275
Time, seconds

a

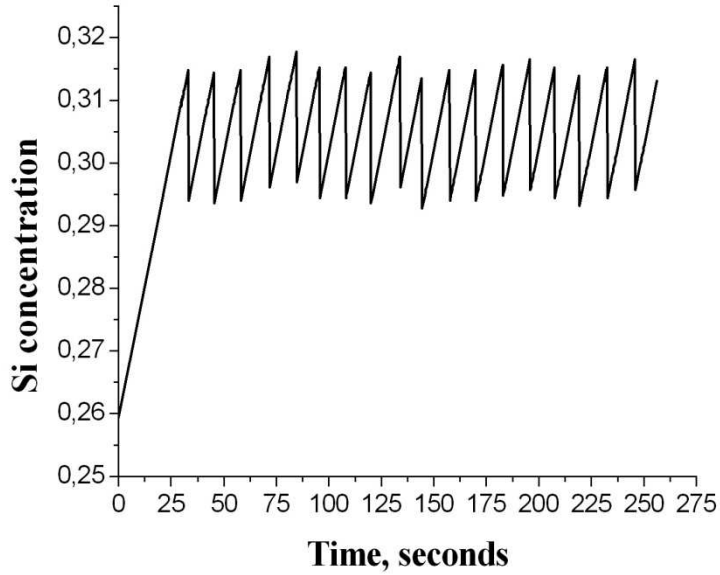
Si concentration
0,32
0,31
0,30
0,29
0,28
0,27
0,26
0,25
0 25 50 75 100 125 150 175 200 225 250 275
Time, seconds

b

Figure 5

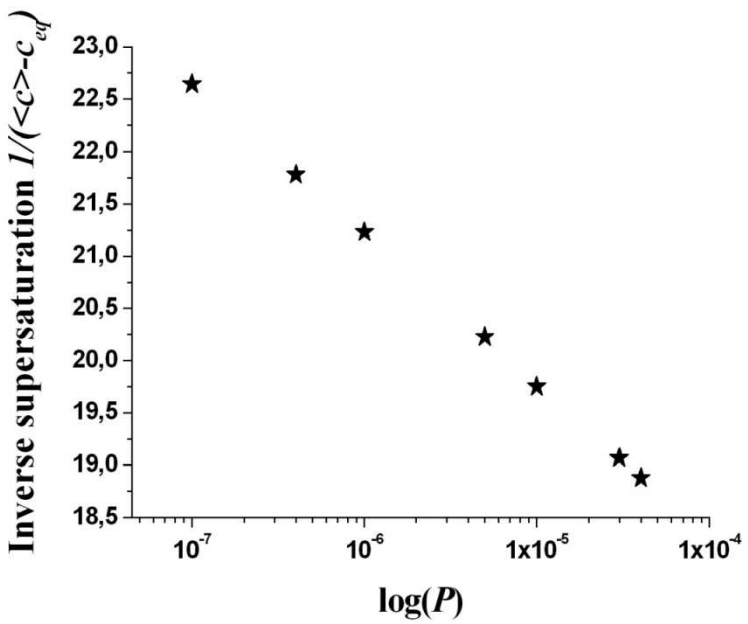
Inverse supersaturation $1/(<c>-c_{eq})$
23,0
22,5
22,0
21,5
21,0
20,5
20,0
19,5
19,0
18,5
10^{-7}
10^{-6}
1x10^{-5}
1x10^{-4}
log(P)

Figure 6

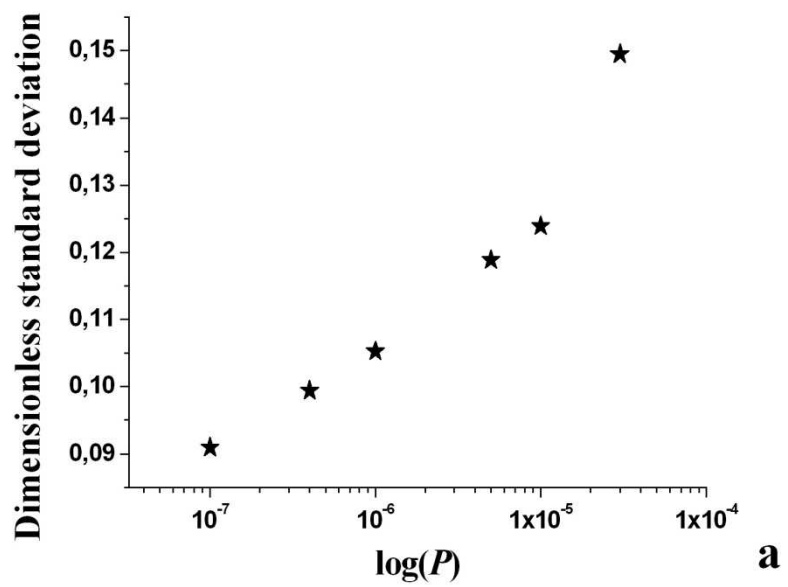
Dimensionless standard deviation
0,15
0,14
0,13
0,12
0,11
0,10
0,09
10-7
10-6
1x10-5
1x10-4
log(P)
a

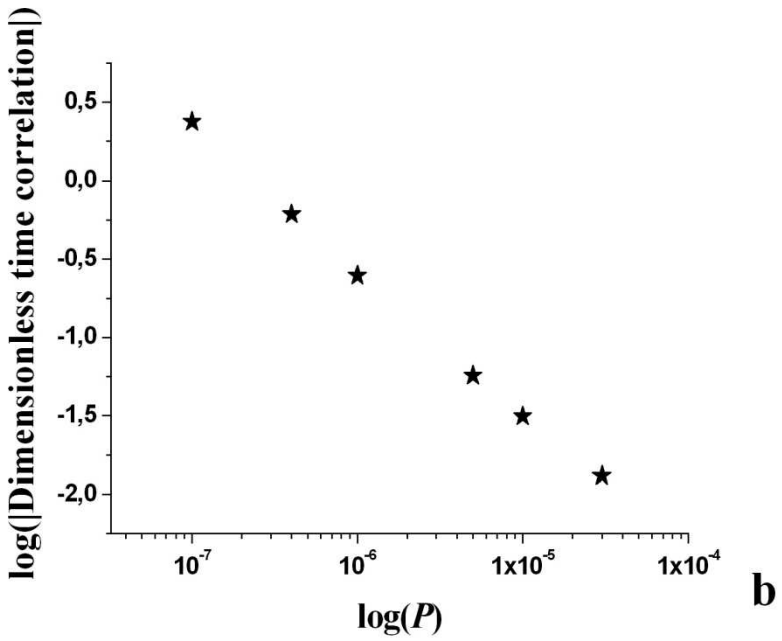
log(|Dimensionless time correlation|)
0,5
0,0
-0,5
-1,0
-1,5
-2,0
10-7
10-6
1x10-5
1x10-4
log(P)
b

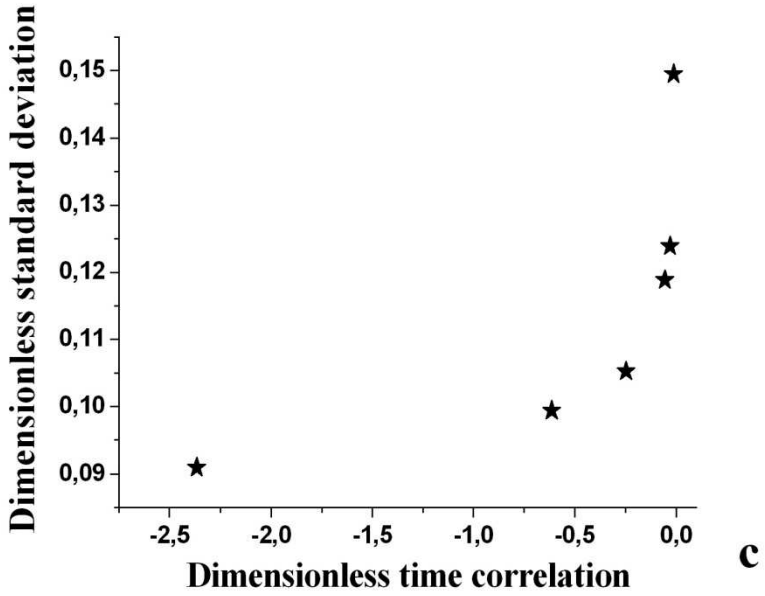
Dimensionless standard deviation
0,15
0,14
0,13
0,12
0,11
0,10
0,09
-2,5
-2,0
-1,5
-1,0
-0,5
0,0
Dimensionless time correlation
c

Figure 7

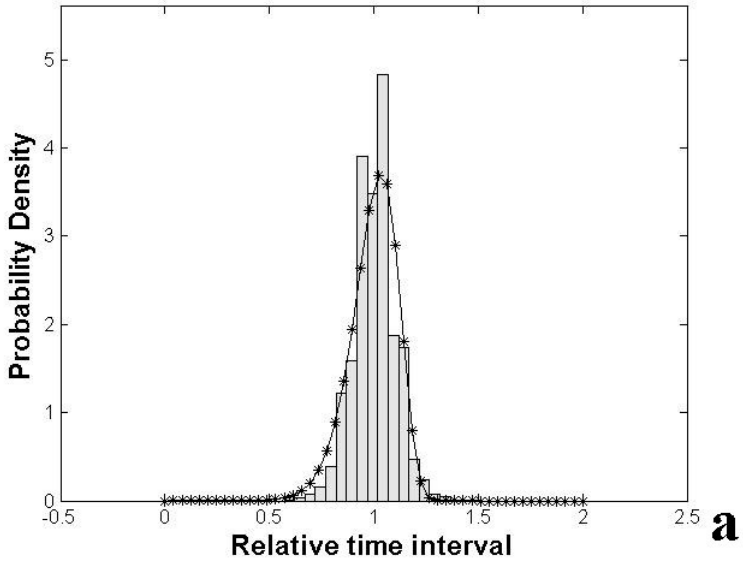
Probability Density
Relative time interval
a

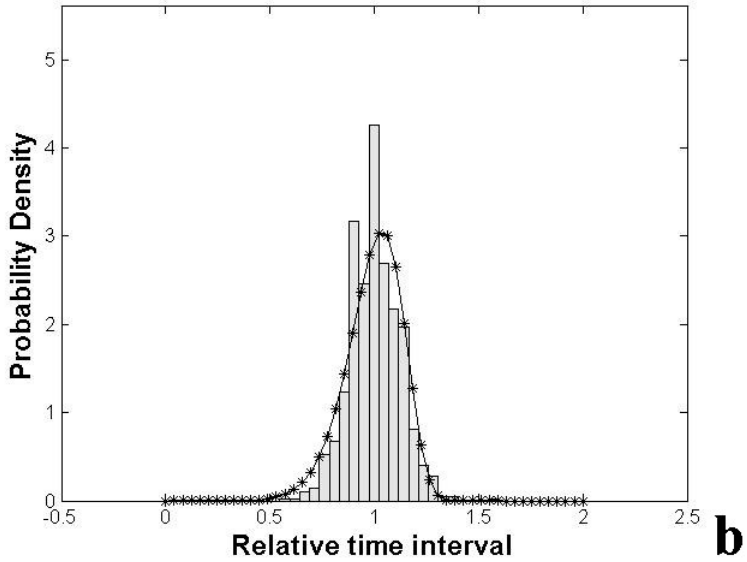
Probability Density
Relative time interval
b

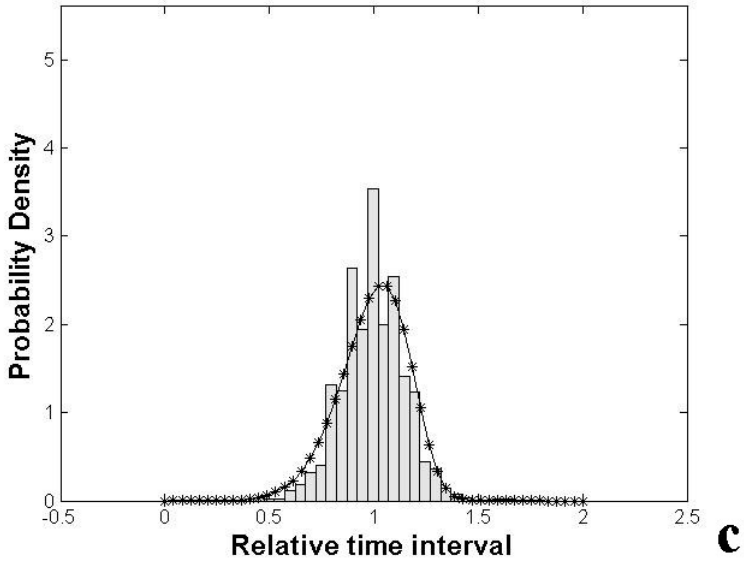
Probability Density
Relative time interval
c

Figure 8

Table 1. Minimal and maximal values of nucleation barriers for $T = 823$ K

Disilane pressure, Torr	Average concentration	Average supersaturation	$\frac{\Delta G_{min}}{kT}$	$\frac{\Delta G_{max}}{kT}$
$4 \cdot 10^{-7}$	0,3053	0,04591	27,762	36.278
$5 \cdot 10^{-6}$	0,3088	0,04944	25,255	36,274
$3 \cdot 10^{-5}$	0,3118	0,05244	23,573	35,319

Table 2. Dependence of different time characteristics on the disilane pressure (T =823K).

Disilane pressure, Torr	Average waiting time, s	Average squared deviation, s	Dimensionless standard deviation	Absolute time correlation, s	Dimensionless time correlation
$4 \cdot 10^{-7}$	12,456	1,238	0,099	-0,759	-0,613
$5 \cdot 10^{-6}$	0,996	0,118	0,119	-0,007	-0,057
$3 \cdot 10^{-5}$	0,166	0,025	0,149	$-3{,}2 \cdot 10^{-4}$	-0,013